Cathepsin B contributes to TNF-α–mediated hepatocyte apoptosis by promoting mitochondrial release of cytochrome *c*

M. Eugenia Guicciardi,[1] Jan Deussing,[2] Hideyuki Miyoshi,[1] Steven F. Bronk,[1] Phyllis A. Svingen,[3] Christoph Peters,[2] Scott H. Kaufmann,[3] and Gregory J. Gores[1]

[1]Division of Gastroenterology and Hepatology, Mayo Medical School, Clinic, and Foundation, Rochester, Minnesota, USA
[2]Institut für Molekulare Medizin und Zellforschung, Albert-Ludwigs-Universität Freiburg, Freiburg, Germany
[3]Division of Oncology Research, Mayo Medical School, Clinic, and Foundation, Rochester, Minnesota, USA

Address correspondence to: Gregory J. Gores, Division of Gastroenterology and Hepatology, Mayo Medical School, Clinic, and Foundation, 200 First Street SW, Rochester, Minnesota 55905, USA.
Phone: (507) 284-0686; Fax: (507) 284-0762; E-mail: gores.gregory@mayo.edu.

TNF-α–induced apoptosis is thought to involve mediators from acidic vesicles. Cathepsin B (cat B), a lysosomal cysteine protease, has recently been implicated in apoptosis. To determine whether cat B contributes to TNF-α–induced apoptosis, we exposed mouse hepatocytes to the cytokine in vitro and in vivo. Isolated hepatocytes treated with TNF-α in the presence of the transcription inhibitor actinomycin D (AcD) accumulated cat B in their cytosol. Further experiments using cell-free systems indicated that caspase-8 caused release of active cat B from purified lysosomes and that cat B, in turn, increased cytosol-induced release of cytochrome *c* from mitochondria. Consistent with these observations, the ability of TNF-α/AcD to induce mitochondrial release of cytochrome *c*, caspase activation, and apoptosis of isolated hepatocytes was markedly diminished in cells from *CatB*$^{-/-}$ mice. Deletion of the *CatB* gene resulted in diminished liver injury and enhanced survival after treatment in vivo with TNF-α and an adenovirus construct expressing the IκB superrepressor. Collectively, these observations suggest that caspase-mediated release of cat B from lysosomes enhances mitochondrial release of cytochrome *c* and subsequent caspase activation in TNF-α–treated hepatocytes.

J. Clin. Invest. **106**:1127–1137 (2000).

Introduction

TNF-α induces apoptosis in a number of different cell types (1). This phenomenon is of particular interest in many human diseases. In the liver, for example, TNF-α–induced apoptosis is thought to contribute to ischemia/reperfusion injury, alcoholic and viral hepatitis, and injury from hepatotoxins (2–5). Information on signaling of apoptosis by this cytokine may lead to therapeutic strategies for the treatment of these liver diseases.

TNF-α–induced apoptosis is mediated by the TNF receptor–1 (TNFR-1). Engagement of TNFR-1 by TNF-α causes receptor oligomerization (6, 7), which results in recruitment of the adapter protein TNFR-associated protein with death domain (TRADD) (8, 9). TRADD then binds Fas-associated protein with death domain (FADD) (10, 11), which in turn binds to and promotes the activation of caspase-8, one of the initiator apoptotic proteases (12–14). However, TNFR-1 is also involved in other interactions. First, TNFR-1 has been reported to activate procaspase-2 through the binding of TRADD to the adapter molecules RIP (receptor-interacting protein) and RAIDD (RIP-associated ICE-homologous protein with death domain) (15). Second, through the binding of TRADD to the downstream transducer TNF-associated factor–2 (TRAF-2) and the protein kinase NF-κB–inducing kinase (NIK), TNFR-1 also activates the transcription factor NF-κB, which activates transcription of polypeptides such as cIAP1 and cIAP2 that antagonize the FADD-mediated death signals (16). As a consequence of this latter pathway, many cells fail to undergo TNF-α–induced cell death unless inhibitors of the NF-κB pathway (e.g., protein synthesis inhibitors, RNA transcription inhibitors, or the IκB superrepressor) are included (17, 18).

Additional studies have raised the possibility that TNF-α might trigger apoptosis through a third pathway involving acidic vesicles. TNF-α signaling has been linked to the activation of acid sphingomyelinase, an enzyme present in acidic vesicles (19). Acid sphingomyelinase generates ceramides, lipid second messengers that have been previously implicated as effectors in TNF-α–mediated apoptosis (20–22). Consistent with this model, agents that alkalinize acidic vesicles have been observed to attenuate TNF-α–induced apoptosis (23). On the basis of these results, Monney and coworkers have implicated unknown lysosomal mediators of TNF-α–initiated apoptotic signaling pathways (23).

Cathepsin B (cat B), a lysosomal cysteine protease, is a candidate for an apoptotic mediator originating from acidic vesicles. Cat B is synthesized as a 38-kDa zymo-

gen that undergoes sequential processing steps within lysosomes. First, a 30-kDa mature active form is generated by proteolytic cleavage (24). Further processing involves removal of the NH_2-terminal propeptide, cleavage of six residues from the COOH-terminus, and internal excision of residues 127 and 128 to generate a two-chain (a 27-kDa heavy chain and a 4- to 5-kDa light chain) form of the enzyme with interchain disulfide bonds. We have previously demonstrated that cat B contributes to bile salt–induced hepatocyte apoptosis by a caspase-8–dependent process (25–27). Studies from other laboratories have also implicated cat B in apoptosis. Pharmacologic inhibition of cat B has been reported to block apoptosis induced by p53 and cytotoxic agents (28). Redistribution of cat B from vesicles to the cytosol has also been demonstrated in neurons undergoing death after global ischemia (29, 30). In a cell-free system, cat B causes chromatin condensation, a morphological feature of apoptosis (31). Based on these previous observations, the goal of the present study was to examine the role of cat B in TNF-α–induced apoptosis.

Methods

Isolation and culture of mouse hepatocytes; culture of McNtcp.24 cells. Cat B knockout (*catB$^{-/-}$*) mice were generated as reported previously (32). Immunoblot analysis demonstrated absence of cat B in *catB$^{-/-}$* mice as well as similar levels of cathepsins D, L and S in *catB$^{-/-}$* vs. *catB$^{+/+}$* mouse hepatocytes. Littermate *catB$^{+/+}$* mice were used as controls. Animals were cared for using protocols approved by the Mayo Clinic Institutional Animal Care and Use Committee. Mouse hepatocytes were isolated and cultured as described by us in detail previously (27). The rat hepatoma McNtcp.24 cell line was cultured as described previously (26). When cells were treated with TNF-α (28 ng/ml), AcD (0.2 μg/ml) was included in the medium to block the NF-κB–mediated transcription of cytoprotective TNF-α–induced genes (33).

Measurement of intracellular cat B activity. Single-cell intracellular cat B–like activity was measured using the fluorogenic protease substrate Z-Val-Leu-Lys-CMAC (VLK-CMAC) and digitized fluorescence microscopy as described previously (26).

Cat B-green fluorescent protein transfection and confocal microscopy. The rat cat B-green fluorescent protein (cat B-GFP) expression vector described previously (25) and a vector encoding the viral protein CrmA were transfected into McNtcp.24 cells using lipofectamine. Confocal microscopy was performed with an inverted Zeiss Laser Scanning Confocal Microscope (Zeiss LSM 510; Carl Zeiss Inc., Thornwood, New Jersey, USA) as described previously (25).

Quantitation of apoptosis. Apoptosis was quantitated by assessing the following: (a) nuclear changes indicative of apoptosis (i.e., chromatin condensation, nuclear fragmentation) using the DNA binding dye 4′,6-diamidino-2-phenylindole (DAPI) dihydrochloride; and (b) externalization of phosphatidylserine (PS) residues using FITC-labeled Annexin V. Glass coverslips containing adherent cells were washed with ice-cold PBS and placed in a custom-made chamber for viewing by an inverted fluorescence microscope. Cells were incubated in 200 μl of binding buffer (10 mM HEPES [pH 7.4], 150 mM NaCl, 5 mM KCl, 1 mM $MgCl_2$, and 1.8 mM $CaCl_2$) containing 2 μl FITC-labeled Annexin V and 5 μg DAPI for 15 minutes at room temperature in the dark. After incubation, cells were viewed by fluorescence microscopy (Nikon Eclipse TE200; Nikon Corp., Tokyo, Japan) using excitation and emission filters of 380 and 430 nm for DAPI, and 490 and 515 nm for FITC. At least 300 cells in six different high-power fields were counted for each treatment by an individual blinded to the experimental conditions.

Adenoviral infection. The recombinant replication-deficient adenovirus Ad5IκB, containing an IκB in which serines 32 and 36 are mutated to alanine (a generous gift of D.A. Brenner, University of North Carolina at Chapel Hill, Chapel Hill, North Carolina, USA), and Ad5ΔE1, an empty adenovirus for control experiments, were grown and purified by banding twice in CsCl gradients as described previously (34). Six hours after the hepatocyte isolation, the medium was changed to DMEM containing 2% FBS, and Ad5IκB or Ad5ΔE1 viral stock solutions were added to the medium at a multiplicity of infection of 20. After rotating the culture dishes every 15 minutes for 2 hours, DMEM supplemented with 12% serum was added for 12–16 hours before cells were exposed to TNF-α.

Immunoblot analysis for caspase activation. Immunoblot analysis was performed using whole-cell lysates as described in detail by Martins et al. (35). Membranes were probed with the following primary antibodies: rabbit anti–caspase-8 serum (a kind gift from A. Srinivasan, IDUN Pharmaceuticals, La Jolla, California, USA); rabbit antiserum raised against the peptide IETD, which corresponds to an epitope at the COOH terminus of the caspase-3 large subunit and is detectable only upon caspase activation (ref. 36; kindly provided by T. Chilcote, Elan Pharmaceuticals, South San Francisco, California, USA); rabbit antiserum raised against the peptide PEPD, which corresponds to an epitope at the COOH terminus of the caspase-9 large subunit and is detectable only upon caspase activation (36); rabbit anti-PARP antiserum (kindly provided by G. Poirier, Laval University, Ste. Foy, Quebec, Canada); mouse monoclonal anti-GRP78 (StressGen, Victoria, British Columbia, Canada); mouse monoclonal anti-lamin A/C antibody (kindly provided by F. McKeon, Harvard University, Cambridge, Massachusetts, USA); chicken anti-lamin B_1 antiserum (37); goat anti-actin polyclonal antibody (Santa Cruz Biotechnology Inc., Santa Cruz, California, USA); or chicken anti-B23 antiserum (38). Immunoblots were developed using ECL enhanced chemiluminescence reagents (Amersham Pharmacia Biotech, Buckinghamshire, United Kingdom) after incubation with horseradish peroxidase–conjugated secondary antibodies.

Immunoblot analysis of cytosolic cat B, cytochrome c, and caspase-8. Cytosolic extracts were prepared by a selective digitonin permeabilization technique established and validated by Leist et al. (39). The extracts were subjected to SDS-polyacrylamide gel electrophoresis as indicated in the various figure legends, transferred to nitrocellulose, and probed with goat polyclonal anti–cat B antiserum (Santa Cruz Biotechnology Inc.), mouse monoclonal anti–cytochrome *c* antibody (PharMingen, San Diego, California, USA), rabbit anti-human caspase-8 antiserum, mouse monoclonal anti–cytochrome *c* oxidase (subunit IV; Molecular Probes Inc., Eugene, Oregon, USA), or goat anti-β-actin, using the method outlined earlier here.

Preparation of subcellular fractions. Cytosolic extracts (S-100) were prepared from mouse hepatocytes using the approach described by Yang et al. (40). Highly purified lysosomes free of mitochondria were isolated from mouse liver as described elsewhere (41, 42). The lysosomal fraction was free of mitochondrial contamination as verified by electron microscopy and by immunoblot analysis for cytochrome *c* oxidase (data not shown). Mitochondria, free of lysosomal contamination, were purified from mouse liver as described by us in detail previously (43).

Cell-free assays. To assay for caspase-8–mediated release of cat B from lysosomes, aliquots of isolated lysosomes (10 μg protein) were treated with 20 ng of active recombinant human caspase-8 or 10–25 ng of purified rabbit m-calpain, in the presence or in the absence of mouse hepatocyte S-100 (50 μg) and the caspase inhibitor Z-VAD-fmk (20 μM), in a final volume of 50 μl of buffer B (220 mM mannitol, 68 mM sucrose, 20 mM HEPES-KOH [pH 7.5], 10 mM KCl, 1.5 mM $MgCl_2$, 1 mM EDTA, 1 mM EGTA, 1 mM dithiothreitol, and 0.1 mM PMSF). To avoid chelating calcium, EGTA and EDTA were omitted from experiments that used calpain. After incubation at 37°C for 1 hour, the reaction mixture was centrifuged at 15,000 *g* for 30 minutes at 4°C to pellet the lysosomes. A 30-μl portion of each supernatant was subjected to SDS-PAGE and probed with anti–cat B antibody as already described here.

To assay for mitochondrial release of cytochrome *c*, a slight modification of the technique described by Luo et al. (44) was used. Briefly, aliquots of isolated mitochondria (25 μg protein) were treated with increasing concentrations of purified cat B (5–50 ng) or purified m-calpain (10 ng), in the presence or in the absence of mouse hepatocyte S-100 (50 μg protein) in a final volume of 50 μl buffer B. After a 1-hour incubation at 37°C, the reaction mixture was sedimented at 12,000 *g* for 5 minutes at 4°C to pellet the mitochondria. A 30-μl aliquot of each supernatant was subjected to SDS-PAGE. After transfer to nitrocellulose, samples were probed with monoclonal anti–cytochrome *c* antibody. To exclude mitochondrial contamination in the supernatants, blots were reprobed with mouse monoclonal anti–cytochrome *c* oxidase. Immunoblots were quantitated by densitometry (Bio-Rad GS-700 Imaging Densitometer equipped with Molecular Analysis software; version 2.1; Bio-Rad Laboratories Inc., Hercules, California, USA) assuming linearity of the signal.

In vivo study. catB$^{+/+}$ and catB$^{-/-}$ mice were injected via the tail vein with either the recombinant replication-deficient adenovirus Ad5IκB encoding IκB superrepressor (0.35×10^9 pfu/mouse in 0.22 ml sterile saline), the control adenovirus Ad5ΔE1 (0.35×10^9 pfu/mouse in 0.22 ml sterile saline), or sterile saline (0.22 ml). Twenty-four hours after the viral injection, mice were injected intravenously with recombinant mouse TNF-α diluted in pyrogen-free saline (0.5 μg/mouse). Two to four hours later, the mice were subjected to deep ether anesthesia. Blood samples from the intrahepatic vena cava and liver tissue were procured. The liver specimens were fixed and stained with H&E using standard histological techniques.

Statistical analysis. All data represent at least three independent experiments using cells from three separate isolations and are expressed as the mean ± SEM. Differences between groups were compared using an unpaired two-tail *t* test.

Reagents. Annexin V-FITC kit was from Trevigen Inc. (Gaithersburg, Maryland, USA). Peroxidase-conjugated goat anti-rabbit IgG, goat anti-mouse IgG, goat anti-chicken IgG, and swine anti-goat IgG were from Biosource International (Camarillo, California, USA). Active recombinant human caspases 8 and 2 were from PharMingen. Human recombinant TNF-α, AcD, purified cat B from bovine spleen, purified Ca^{2+}-dependent protease (m-calpain) from rabbit muscle, DAPI, BSA, PMSF, aprotinin, pepstatin, leupeptin, a kit for serum alanine aminotransferase assay, and all other chemicals used were from Sigma Chemical Co. (St. Louis, Missouri, USA).

Results

Is cat B translocated to cytosol during treatment of mouse hepatocytes with TNF-α/AcD? In initial experiments, cultured hepatocytes were treated with 28 ng/ml TNF-α plus 0.2 μg/ml AcD for 4 hours, then assayed for intracellular cat B activity in situ using the fluorogenic substrate VLK-CMAC and digitized video microscopy (Figure 1a). As expected, no significant cat B activity was detected in hepatocytes from catB$^{-/-}$ mice. In contrast, a 4.5-fold increase in intracellular hydrolysis of VLK-CMAC was observed in treated catB$^{+/+}$ mouse hepatocytes compared to untreated cells. Because this substrate is impermeant to lysosomes, these data suggested that cytosolic cat B activity was increased after treatment of mouse hepatocytes with TNF-α/AcD.

To determine whether the increase in cytosolic cat B activity was due to release of cat B from lysosomes, we searched for cat B in cytosol by immunoblot analysis (Figure 1b). Cat B active fragments p30 and p27 increased in the cytosol of catB$^{+/+}$ cells after 8 hours of treatment (lane 3), providing further evidence that TNF-α induces cat B release from lysosomes into the cytosol.
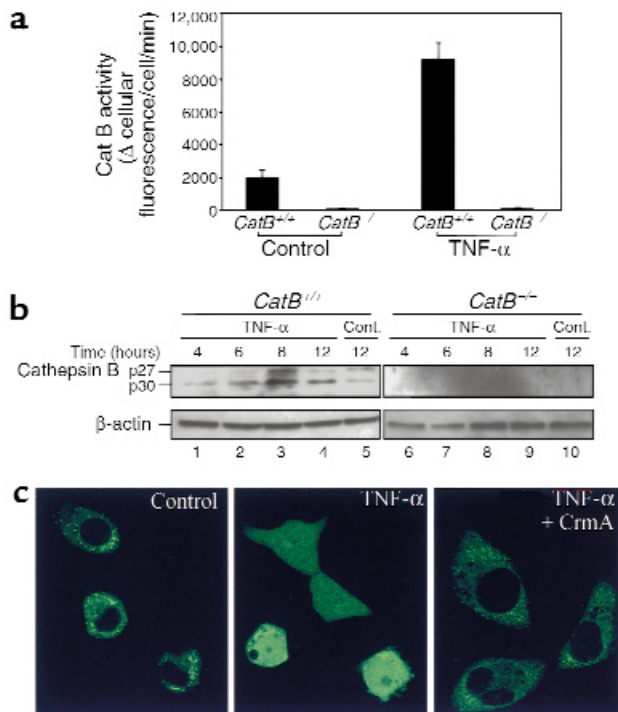
Figure 1

Cat B contributes to TNF-α/AcD–induced hepatocyte apoptosis. Isolated hepatocytes from *catB+/+* and *catB–/–* mice were incubated in the absence (control) or presence of TNF-α (28 ng/ml) and AcD (0.2 µg/ml) for up to 12 hours. (**a**) Intracellular cat B activity was measured fluorometrically in the cells after 4 hours of treatment using the fluorogenic substrate VLK-CMAC and digitized video microscopy, as described in Methods. (**b**) At the indicated time points, cytosolic extracts were prepared by selective permeabilization with digitonin as described in Methods and subjected to immunoblot analysis using an anti–cat B antiserum. Locations of 30-kDa (p30) and 27-kDa (p27) active fragments of cat B are indicated. Immunoblot analysis of β-actin was performed as a control for protein loading. Cont., control. (**c**) Cultured McNtcp.24 cells grown on collagen-coated glass coverslips were transfected with the plasmid construct encoding the cat B-GFP fusion protein (control, TNF-α) or double-transfected with the cat B-GFP plasmid and the plasmid encoding the viral protein CrmA (CrmA + TNF-α). Forty-eight hours later, cells were incubated in the absence (control) or presence of TNF-α/AcD at 37°C for 2 hours and transferred to the stage of an inverted confocal microscope. Cat B-GFP fluorescence was imaged as described in Methods.

To provide independent evidence for the proposed translocation of cat B from lysosomes to cytosol during TNF-α–induced apoptosis, confocal microscopy was used to visualize directly the cellular compartmentation of expressed cat B-GFP in transfected McNtcp.24 cells (Figure 1c). In untreated cells, the distribution of the cat B-GFP fusion protein was punctate and only localized in the cytosol. After treatment with TNF-α/AcD, the fluorescence was diffusely distributed in the cytoplasm and was also clearly identified in the nuclear region. These data are consistent with translocation of cat B from a vesicular compartment into the cytoplasm during exposure to TNF-α/AcD.

Do proximal caspases promote release of cat B from lysosomes? Because TNFR-1 appears to initiate apoptotic signaling by activating caspases (11, 15), we sought to determine whether proximal caspases could directly promote release of cat B from lysosomes. We addressed this question by (a) transfecting McNtcp.24 cells using CrmA, a specific caspase-8 inhibitor, and assessing the distribution of cat B-GFP; and (b) using a cell-free system to determine whether caspase-8 will directly cause release of cat B from lysosomes. After transfection with CrmA, release of cat B-GFP from lysosomes was inhibited in TNF-α/AcD–treated McNtcp.24 cells (Figure 1c). In the cell-free system, isolated lysosomes were incubated with different concentrations of active recombinant caspase-8 in the presence or in the absence of cytosol. After the lysosomes were sedimented, supernatants were analyzed for cat B (Figure 2a). Active caspase-8 directly induced a release of cat B from lysosome (Figure 2a, lane 2) corresponding to about 26% of the maximum release obtained treating the lysosomes with the detergent Triton X-100 (Figure 2b, lane 6). The release was markedly enhanced to 82% by the presence of cytosol (Figure 2a, lane 3) and was almost completely blocked (6%) by the broad-spectrum caspase inhibitor Z-VAD-fmk (Figure 2a, lane 4), confirming that the catalytic activity of the recombinant caspase-8 was necessary for this phenomenon. Similar results were also observed with another potential proximal caspase, recombinant caspase-2 (data not shown). As a protease control for these experiments, we chose m-calpain, a cytosolic cysteine protease that has been implicated in apoptosis (45) and has been
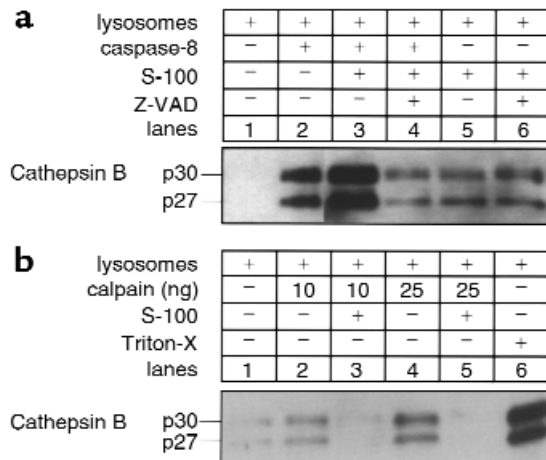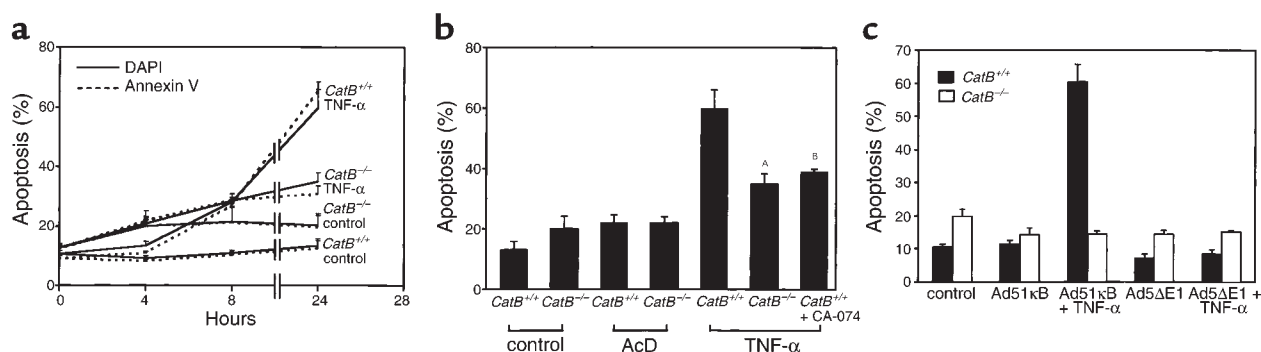

Figure 2

Caspase-8 induces release of cat B from lysosomes. Isolated lysosomes from *catB+/+* mouse liver (10 µg protein) were incubated at 37°C with either active recombinant human caspase-8 (20 ng) (**a**) or rabbit m-calpain (10–25 ng) (**b**), in the absence or presence of S-100 cytosol fraction (50 µg protein) and the caspase inhibitor Z-VAD-fmk (20 µM). Lysosomes were also treated with 0.1% Triton-X 100 to induce maximal release of cat B (positive control). After 1 hour, lysosomes were pelleted by centrifugation at 15,000 *g* for 30 minutes. Supernatants were subjected SDS-PAGE on gels containing 10% acrylamide, transferred to nitrocellulose, and probed with anti–cat B antiserum.

shown to be activated by TNF-α (46). Although addition of calpain to the cell-free system induced release of cat B from lysosomes (Figure 2b, lanes 2 and 4), this release was blocked in the presence of cytosol (Figure 2b, lanes 3 and 5). Thus, the results with calpain were the reverse of those with caspase-8, wherein cytosol potentiated the release of cytochrome *c*. Likely, the presence of calpastatin in the cytosol inhibits the activity of calpain preventing its proteolytic effects on lysosomes in the cell-free system. Coupled with the CrmA results (Figure 1c), these observations suggest caspase specificity for the observed effects and implicate a proximal caspase or a cytosolic caspase substrate in the TNF-α/AcD–induced release of cat B from lysosomes.

Is TNF-α/AcD–induced apoptosis reduced in catB−/− mouse hepatocytes? To determine whether this cytosolic translocation of cat B plays a role in TNF-α–induced hepatocyte apoptosis, we compared the ability of *catB+/+* and *catB−/−* hepatocytes to undergo apoptosis in response to TNF-α + AcD. To quantitate apoptosis, we monitored the nuclear changes by DAPI and the cellular externalization of phosphatidylserine by FITC-annexin V labeling. Both techniques yielded similar results (Figure 3a). Actinomycin D alone did not significantly increase the amount of apoptosis observed in untreated hepatocytes (Figure 3b). In contrast, TNF-α/AcD markedly enhanced *catB+/+* hepatocyte apoptosis (Figure 3, a and b). An increased number of apoptotic cells were first detected between 4 and 8 hours after addition of TNF-α and AcD to *catB+/+* hepatocytes and progressively increased with time until they comprised 59 ± 6% of the total cell population at 24 hours (Figure 3, a and b). TNF-α/AcD–induced apoptosis was reduced by almost half in *catB−/−* cells (35 ± 3% vs. 59 ± 6% after 24 hours of treatment; *P* < 0.05; Figure 3b). A similar decrease was observed when *catB+/+* hepatocytes were treated with TNF-α/AcD in the presence of the highly selective cat B inhibitor, CA-074 (Figure 3b). To exclude the possibility that these results are due to a specific effect of actinomycin D in sensitizing cells to TNF-α (47), we performed similar experiments using expression of an IκB superrepressor to block NF-κB survival signals. Cells were infected with an adenovirus that expressed the superrepressor of IκB (Ad5IκB) or an empty control virus (Ad5ΔE1). Compared with controls, TNF-α–induced apoptosis was completely blocked in *catB−/−* cells (Figure 3c). These results suggest that TNF-α–induced apoptosis is dependent, in part, upon cat B activity.

Does cat B deletion alter TNF-α/AcD–induced caspase activation in mouse hepatocytes? Current concepts implicate caspases as an integral part of the cell death machinery in death receptor–mediated apoptosis. The reduced rates of apoptosis in *catB−/−* hepatocytes suggested that caspase activation might be quantitatively or qualitatively altered by deletion of cat B. To address this possibility, we initially assessed the cleavage of several well-characterized substrates of downstream effector caspases, including PARP; lamins A, B$_1$, and C; and the nucleolar protein B23, by immunoblot analysis. As shown in Figure 4, all of these substrates were completely cleaved in *catB+/+* mouse hepatocytes after a 24-hour treatment with TNF-α/AcD (Figure 4, lane 2). In contrast, cleavage of these substrates was markedly diminished in hepatocytes from *catB−/−* mice (Figure 4, lane 4). These observations suggested that deletion of cat B causes a defect in TNF-α/AcD–induced activation of effector caspases.


Figure 3

catB−/− mouse hepatocytes are more resistant to TNF-α–induced apoptosis. Isolated hepatocytes from *catB+/+* and *catB−/−* mice were incubated in the absence (control) or presence of TNF-α and AcD. (**a**) Apoptosis was quantitated in *catB+/+* and *catB−/−* hepatocytes at different times of incubation after staining with both FITC-annexin V (dotted lines) and DAPI (solid lines). Cells were considered apoptotic if either externalization of phosphatidylserine residues on the plasma membrane or chromatin condensation and nuclear fragmentation occurred. At least 300 cells in six high-power fields were counted by an individual blinded to the experimental conditions. (**b**) Apoptosis was quantitated in *catB+/+* and *catB−/−* hepatocytes by DAPI staining after 24 hours of incubation in medium lacking (control) or containing either TNF-α and AcD (TNF-α) or AcD alone (AcD). *catB+/+* hepatocytes were also treated with TNF-α and AcD after a 30-minute preincubation with CA-074, a pharmacological inhibitor of cat B. Results are representative of at least three independent experiments using cells from three separate isolations and are expressed as mean ± SEM. Data were compared using a one-tail *t* test. [A]*P* < 0.05, *catB−/−* vs. *catB+/+*; [B]*P* < 0.05, *catB+/+* + CA-074 vs. *catB+/+*. (**c**) Isolated mouse hepatocytes from *catB+/+* (filled bars) and *catB−/−* (open bars) mice were infected with an adenovirus expressing the IκB-superrepressor (Ad5IκB) or with an empty adenovirus (Ad5ΔE1) as a negative control, and treated with TNF-α (28 ng/ml) for 12 hours. Apoptosis was quantitated after staining with DAPI. Results are representative of three independent experiments performed in triplicate from separate isolations and are expressed as mean ± SEM.

Figure 4

Cleavage of PARP, lamins, and B23 after TNF-α/AcD treatment is diminished in *catB*−/− hepatocytes. Hepatocytes from *catB*+/+ and *catB*−/− mice were incubated for 24 hours with medium lacking or containing TNF-α + AcD. Whole-cell lysates were then prepared as described in Methods. Aliquots containing 50 μg protein were subjected to SDS-PAGE on gradient gels containing 5–15% acrylamide, transferred to nitrocellulose, and sequentially blotted for PARP, lamins A and C, lamin B₁, or B23. Cleavage of the substrates was detected by the loss of the bands corresponding to the molecular weight of the native protein, and, in the case of B23, by the appearance of a new band (arrow). GRP78 served as a control for protein loading.
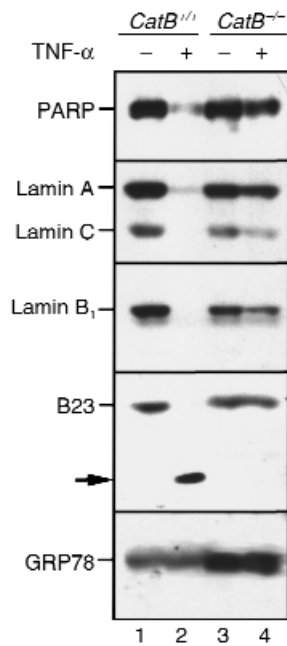

In some cell types, caspase-8–initiated apoptosis occurs by a process associated with mitochondrial release of cytochrome *c* and subsequent activation of caspase-9 (48). To determine whether TNF-α–induced apoptosis involves this pathway in mouse hepatocytes and assess whether cat B was upstream or downstream of mitochondria, the presence of cytosolic cytochrome *c* and activated caspase-9 was evaluated by immunoblotting. Increased cytochrome *c* was detectable in the cytosol of *catB*+/+ mouse hepatocytes beginning 6 hours after addition of TNF-α/AcD (Figure 5a, lane 2). In contrast, no cytochrome *c* was detectable in the cytosol of *catB*−/− cells after TNF-α/AcD treatment for up to 24 hours (Figure 5a, lanes 1–4). Consistent with these data, proteolytically activated caspase-9 (36) was readily detectable in treated *catB*+/+ hepatocytes but not *catB*−/− cells (Figure 5b, lanes 2 and 4). Likewise, activated caspase-3 was observed in *catB*+/+ mouse hepatocytes but not *catB*−/− cells (Figure 5b, lanes 2 and 4).

Taken together, the results in Figure 5 indicate that TNF-α/AcD–induced hepatocyte apoptosis involves mitochondrial release of cytochrome *c* and activation of caspase-9. These events are reminiscent of type II cells as defined by Scaffidi et al. (49, 50). In such cells, the initial activation of caspase-8 is limited and generally below the level of detection. Release of cytochrome *c* and activation of caspase-9 amplifies the original signal, leading to activation of downstream caspases (49, 50). Once these downstream caspases are activated, recent results indicate that they can in turn cleave more procaspase-8 (51). Thus, if TNF-α/AcD–treated hepatocytes were behaving like type II cells, we predicted that (a) the amount of activated caspase-8 would be limited until after caspase-9 was activated, and (b) *catB*−/− cells (which do

not activate caspase-9) would not display detectable caspase-8 activation. Further experiments were performed to test these predictions.

Immunoblot analysis demonstrated that TNF-α/AcD treatment of *catB*+/+ hepatocytes resulted in a time-dependent processing of procaspase-8 (Figure 5b) into the catalytically active subunits of 18–20 kDa (p20) and 10 kDa (p10) (Figure 6). As predicted, detectable processing of procaspase-8 was not evident until 6–8 hours after addition of the cytokine (Figure 6, lanes 2 and 3). Thus, the amount of active caspase-8 required for detection by immunoblot analysis appears to be generated
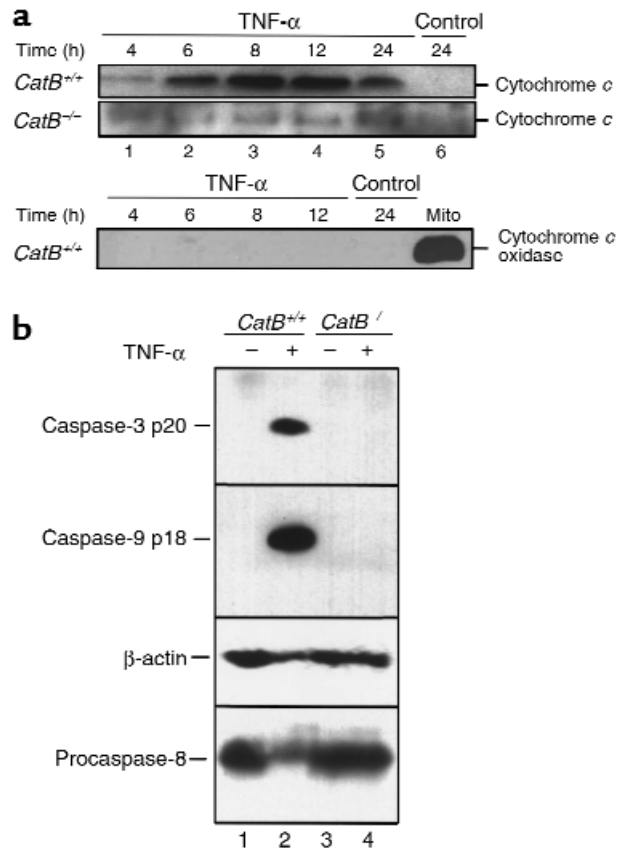
Figure 5

(**a**) TNF-α–induced release of cytochrome *c* into the cytosol is reduced in *catB*−/− mouse hepatocytes. At the indicated times after addition of medium lacking (control) or containing TNF-α + AcD, cytosol fractions were prepared by selective permeabilization with digitonin as described in Methods. Aliquots containing 20 μg of protein were subjected to SDS-PAGE on gels containing 15% acrylamide, transferred to nitrocellulose, and probed for cytochrome *c*. Samples from *catB*+/+ hepatocytes were also probed for cytochrome *c* oxidase, to exclude a possible mitochondrial contamination in the cytosol. (**b**) Caspase-9 and caspase-3 are processed in TNF-α/AcD–treated *catB*+/+ hepatocytes but not in *catB*−/− hepatocytes. Cells were incubated for 24 hours in medium lacking or containing TNF-α + AcD. After whole-cell lysates were prepared as described in Methods, aliquots containing 50 μg protein were subjected to SDS-PAGE, transferred to nitrocellulose membrane, and analyzed by immunoblot using antisera that recognize only active caspase-9 or active caspase-3 (36). The same blot was probed with sera that recognize procaspase-8 and β-actin to confirm loading and transfer of samples from *catB*−/− mice.
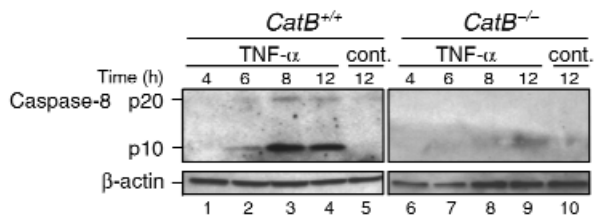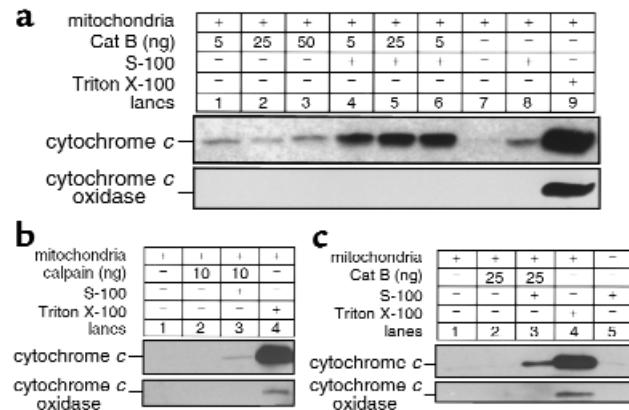
Figure 6
Caspase-8 activation after TNF-α/AcD treatment is reduced in *catB*^{−/−} cells. After cells were incubated in medium without (cont.) or with TNF-α + AcD for the indicated lengths of time, cytosolic fractions were prepared. Aliquots containing 40 μg protein were subjected to SDS-PAGE on gels containing 15% acrylamide, transferred to nitrocellulose, and immunoblotted for caspase-8. Processing of caspase-8 was detected by the appearance of the 18- to 20-kDa (p20) and 10-kDa (p10) active fragments. β-Actin served as a control for protein loading. Results are representative of three independent experiments.

after mitochondrial release of cytochrome *c* (Figure 5a, lane 2), not by direct activation at the TNFR-1–associated signaling complex. Consistent with this conclusion, *catB*^{−/−} hepatocytes, which did not release cytochrome *c*, did not display detectable caspase-8 processing (Figure 5b, lane 4; Figure 6, lanes 6–9).

Does cat B induce release of cytochrome c from mitochondria? The preceding results place cat B upstream of mitochondria in the TNF-α/AcD–induced apoptotic cascade in mouse hepatocytes. Although more complicated models are possible, the most direct model would have cat B or a substrate of cat B inducing cytochrome *c* release from mitochondria. To assess this possibility, purified cat B was incubated with isolated mitochondria in the presence and absence of cytosol. At the end of the incubation, the mitochondria were sedimented and the resulting supernatants analyzed for cytochrome *c*. In the absence of cytosol, active cat B directly induced a moderate release of cytochrome *c* from mitochondria (Figure 7a, compare lanes 1–3 with lane 7) corresponding to about 8% of the maximum release as obtained treating the mitochondria with the detergent Triton X-100 (Figure 7a, lane 9). However, cytochrome *c*–releasing activity of cat B was fivefold greater in the presence of cytosol (Figure 7a, lanes 4–6). Addition of calpain to the cell-free system did not induce release of cytochrome *c* from mitochondria, demonstrating that the release is due to cat B activity and not a nonspecific proteolytic effect (Figure 7b). To rule out the possibility that mitochondria from *catB*^{−/−} might have developed an increased resistance toward cytochrome *c* release, we performed the same experiments using both mitochondria and cytosolic extracts obtained from *catB*^{−/−} hepatocytes. As previously observed in *catB*^{+/+}, active cat B induced release of cytochrome *c* from the mitochondria in the presence of cytosol (Figure 7c, lane 3), demonstrating that the absence of cytochrome *c* release in *catB*^{−/−} is not due to secondary modifications in the mitochondria of these animals. These

data imply the existence of a cytosolic cat B substrate that, after proteolytic activation, is capable of causing release of cytochrome *c* from mitochondria.

Are catB^{−/−} *mice resistant to TNF-α–induced liver damage in vivo? catB*^{+/+} and *catB*^{−/−} mice were injected with the adenovirus Ad5IκB to block the TNF-α–survival pathways signaling through NF-κB. Twenty-four hours later, TNF-α was administered intravenously. At 2 and 4 hours after TNF-α treatment, serum ALT concentrations were significantly higher in *catB*^{+/+} than in *catB*^{−/−} animals (Figure 8a). Livers from the *catB*^{+/+} mice displayed extensive hemorrhagic lesions and numerous clusters of apoptotic cells. In contrast, liver specimens from the *catB*^{−/−} mice showed minimal damage (Figure 8b). Further studies revealed that TNF-α treatment of the *catB*^{+/+} mice was fatal in greater than 80% of animals at 5 hours (*n* = 6), whereas *catB*^{−/−} mice universally survived at least 72 hours after TNF-α treatment (*n* = 4).

Figure 7
Cat B–induced release of cytochrome *c* from mitochondria is enhanced by cytosol and is not due to a nonspecific proteolytic effect. Isolated mitochondria from *catB*^{+/+} mouse liver (25 μg protein) were incubated at 37°C with increasing concentrations of purified recombinant cat B (5–50 ng) (**a**) or m-calpain (10 ng) (**b**), in the presence or in the absence of S-100 cytosol fraction (50 μg) as described in Methods. Mitochondria were also treated with 0.1% Triton X-100 to induce maximum release of cytochrome *c* (positive control). After 1 hour, mitochondria were pelleted by centrifugation at 12,000 *g* for 5 min. Supernatants were subjected to SDS-PAGE on 15% acrylamide gels, transferred to nitrocellulose, and immunoblotted for cytochrome *c*. Blots were also probed for cytochrome *c* oxidase (subunit IV) to exclude mitochondria contamination in the supernatant. (**c**) Active cat B induces release of cytochrome *c* from isolated *catB*^{−/−} mouse liver mitochondria in the presence of cytosol. Isolated mitochondria from *catB*^{−/−} mouse liver (25 μg protein) were incubated at 37°C with purified recombinant cat B (25 ng), in the presence or in the absence of S-100 cytosol fraction (50 μg) obtained from the same animal. Mitochondria were also treated with 0.1% Triton X-100 to induce maximum release of cytochrome *c* (positive control). After 1 hour, mitochondria were pelleted by centrifugation at 12,000 *g* for 5 minutes, and the resulting supernatants were subjected to SDS-PAGE and subsequent immunoblot analysis for cytochrome *c* as already above. Immunoblot for cytochrome *c* oxidase (subunit IV) was also performed to exclude mitochondria contamination in the supernatant.
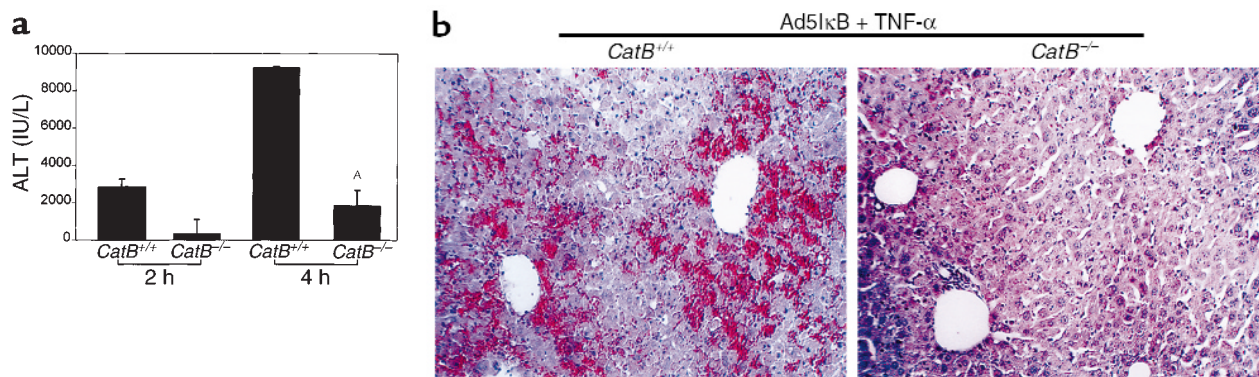
Figure 8

catB^{−/−} mice are more resistant to TNF-α–induced liver damage. *catB*^{−/−} and *catB*^{+/+} were injected via tail vein with the adenovirus Ad5IκB (0.35 × 10⁹ pfu/mouse) encoding for an IκB superrepressor. In control experiments, mice were injected with the adenovirus Ad5ΔE1 (0.35 × 10⁹ pfu/mouse in 0.22 ml sterile saline) or with sterile saline (0.22 ml). Twenty-four hours later, each mouse received a dose of 0.5 μg of recombinant mouse TNF-α intravenously. Mice were sacrificed after 2- and 4-hour treatment with TNF-α. (**a**) Serum alanine aminotransferase (ALT) levels were measured and expressed as mean ± SEM (*n* = 3). $^{A}P < 0.01$. ALT values in control samples were < 20 IU/L, except in the Ad5ΔE1-injected mice, in which they were < 750 IU/L at 2 hours and < 1850 IU/L at 4 hours (data not shown). (**b**) H&E staining of Ad5IκB-injected *catB*^{+/+} (left) and *catB*^{−/−} (right) mouse liver harvested 4 hours after treatment with TNF-α.

Discussion

Cat B is synthesized as a proenzyme and transported into lysosomes, where it is processed and activated either by lysosomal proteases or by autoactivation (52, 53). This compartmentation of cat B within acidic vesicles prevents it from inducing cell injury. However, during treatment of hepatocytes with TNF-α/AcD, increased cat B was detected in cytosol (Figure 1, a and b). Consistent with these results, translocation of GFP-cat B from a vesicular compartment to cytosol was demonstrated during TNF-α/AcD-induced apoptosis (Figure 1c). These observations suggest that cat B is released from lysosomes to the cytosol during TNF-α/AcD–induced apoptosis. Further experiments demonstrated that active caspase-2 or -8 was capable of causing cat B release from purified lysosomes (Figure 2a and data not shown). These data provide a link between an event known to occur at the ligated TNFR-1 (proximal caspase activation) and cat B release.

The detailed mechanism by which cat B is released from lysosomes after caspase treatment is not currently understood. Atractyloside, which is commonly used to induce the mitochondrial permeability transition and release of cytochrome *c* from mitochondria, has been reported to induce release of cat B from isolated lysosomes (31). This observation raises the possibility that similar mechanisms of pore opening might exist in mitochondria and lysosomes, promoting selective or semiselective release of constituents from both organelles during apoptosis. Alternatively, we cannot at present rule out the possibility that cat B release from lysosomes occurs by a totally different process.

To determine whether cat B might play a critical role in the TNF-α–triggered apoptotic cascade, hepatocytes from *catB*^{−/−} and *catB*^{+/+} mice were compared. Apoptosis was diminished in the *catB*^{−/−} cells (Figure 3), suggesting that the cytosolic release of cat B was more than just an epiphenomenon. Furthermore, *catB*^{−/−} mice were resistant to liver injury and had improved survival after TNF-α treatment (Figure 8). These observations prompted us to search for a potential role of cat B in apoptotic cellular events.

Previous studies have suggested that cathepsins can activate certain caspases. Cathepsin G (a serine protease), for example, directly activates caspase-7 (54). Cat B has been reported to activate the proinflammatory caspase-11 and, to a lesser extent, caspase-1 (31, 55). These same studies, however, demonstrated that cat B cannot process the effector caspases 3, 6, and 7 (31, 55). Accordingly, we sought a different explanation for the decreased activation of effector caspases observed in *catB*^{−/−} cells (Figures 4 and 5).

Scaffidi et al. have identified two different apoptosis signaling pathways originating from the Fas death receptor complex and proposed a classification for cells into type I or type II (49). In type I cells, Fas receptor ligation activates large amounts of caspase-8, which then directly activates caspase-3 in a mitochondria-independent pathway. In contrast, type II cells generate reduced amounts of active caspase-8 and rely on a mitochondria-dependent amplification step to achieve caspase-3 activation. Hepatocytes are type II cells (56). Although a similar distinction between type I and type II cells has not been previously reported in the context of TNF-α–induced apoptosis, release of cytochrome *c* from mitochondria has been reported in a number of cell types after TNF-α treatment (57, 58). Our data suggest that TNF-α–treated hepatocytes behave like type II cells. In particular, we observed release of cytochrome *c* from mitochondria and activation of caspase-9 in these cells. In addition, we observed that active caspase-8 was detectable by immunoblotting (Figure 6) only after release of cytochrome *c* to the cytosol (Figure 5a). These observations suggest that large amounts of cas-

pase-8 are processed at a step downstream of mitochondria in TNF-α–treated hepatocytes, as occurs in other type II cells (49, 50, 59).

Further experiments were performed to determine how cat B might be affecting this apoptotic cascade in TNF-α–treated hepatocytes. We observed that the appearance of cytochrome *c* in cytosol of TNF-α–treated wild-type mouse hepatocytes occurred with a time course similar to that of cat B release from lysosomes (Figures 1b and 5a). Moreover, cytochrome *c* release, caspase-9 activation, and caspase-3 activation were marked diminished in *catB$^{-/-}$* cells (Figure 5). These observations place cat B upstream of mitochondria in this type II pathway and provide an alternative mechanism by which cat B can affect activation of effector caspases.

To test the hypothesis that cat B directly causes mitochondrial release of cytochrome *c*, we evaluated release of cytochrome *c* from purified mitochondria. Although purified cat B induced cytochrome *c* release in this cell-free system, the release was markedly enhanced in the presence of cytosol (Figure 7), suggesting that one or more cytosolic targets of cat B might be responsible. Similar observations have been reported for the cytochrome *c*–releasing activity of caspase-8 (59, 60). Bid, a BH3 domain-containing Bcl-2 family member located in the cytosol, is cleaved by caspase-8 (44, 61, 62). Upon cleavage, the COOH-terminal fragment translocates to mitochondria and triggers cytochrome *c* release. Although Bid would appear to be a potential candidate for cat B–mediated apoptosis, the current lack of suitable reagents to evaluate Bid cleavage in mouse cells precluded direct evaluation of this possibility.

Collectively, the data from the present study appear to define an apoptotic pathway that involves the ligated TNFR-1 complex as well as constituents of lysosomes, mitochondria, and cytosol. In particular, our results point to a model (Figure 9) that involves the following steps: binding of TNF-α with its receptor, activation of a proximal caspase at a TNFR-1–associated death-inducing signaling complex (DISC), caspase induced release of cat B from lysosomes, cat B–induced cleavage of a currently unknown cytosolic substrate, induction of cytochrome *c* release from mitochondria by cat B and the cleaved cytosolic substrate, activation of caspase-9, and activation of effector caspases. The steps leading to proximal caspase activation are well documented in previous studies (1, 63); the present study provides evidence for all the postulated steps downstream of proximal caspase activation at the DISC. Although other death receptors such as Fas are associated with caspase-8 activation, hepatocyte apoptosis was not reduced in *catB$^{-/-}$* cells treated with the agonistic Jo2 antisera (data not shown). This observation suggests that there are differences in apoptotic signaling pathways between death receptors even in the same cell type.

Cathepsin D, a lysosomal aspartyl protease, has also been implicated in apoptosis by cytokines and oxidative stress (64, 65). These previous studies and our current data support the concept of a lysosomal pathway in apoptosis. Whether lysosomal proteases are released specifically in different cell types by specific apoptotic triggers or there is a generalized release of lysosomal proteases into the cytosol will require further study. However, cathepsin D and B have markedly different substrate specificities, and their effects in proteolytic cascades would be predicted to be different.

Although it is tempting to speculate that this acidic vesicle pathway might be important in amplifying TNF-α–initiated death signals in type II cells such as hepatocytes, further studies are required to evaluate its true physiological importance. Like TNFR-1 knockout mice (66), *catB$^{-/-}$* mice develop normally and have no overtly manifest phenotype. Moreover, *catB$^{-/-}$* hepatocytes were not totally resistant to TNF-α–induced apoptosis, raising the possibility that an additional apoptotic pathway is also activated in hepatocytes by this cytokine. This additional pathway does not appear to involve caspase-3 (Figure 5b, lane 4), but may instead be mediated by the recently described FADD-dependent, caspase-8–independent mechanism of cell death (67, 68). Nonetheless,
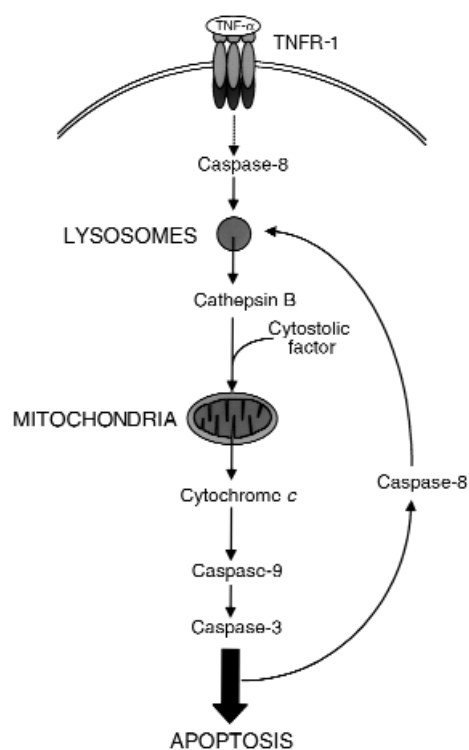
Figure 9
Model of TNF-α signaling pathway through acidic compartment. Triggering of TNFR-1 leads to activation of a small amount of caspase-8, sufficient to induce the release of cat B from the lysosomes. Active cat B in turn promotes the release of cytochrome *c* from mitochondria by cleaving one or more still unidentified cytosolic substrates. Release of cytochrome *c* results in cleavage of caspase-9 and caspase-3 followed by further apoptotic changes. Strong activation of caspase-8 occurs downstream of mitochondria, possibly by effector caspases. An amplification loop might generate more active caspase-8, inducing further release of cat B from lysosomes.

the present demonstration that TNF-α–induced liver injury and death are diminished in *catB*$^{-/-}$ mice suggests the potential importance of the cat B–mediated pathway. Further studies using various models of liver injury should not only provide a more complete picture of the role of cat B in this process, but also evaluate cat B as a potential therapeutic target for reducing inflammation-induced hepatocellular damage.

1. Wallach, D., et al. 1999. Tumor necrosis factor receptor and Fas signaling mechanisms. *Annu. Rev. Immunol.* **17**:331–367.
2. Colletti, L.M., et al. 1990. Role of tumor necrosis factor-alpha in the pathophysiologic alterations after hepatic ischemia/reperfusion injury in the rat. *J. Clin. Invest.* **85**:1936–1943.
3. McClain, C.J., and Cohen, D.A. 1989. Increased tumor necrosis factor production by monocytes in alcoholic hepatitis. *Hepatology.* **9**:349–351.
4. Gonzalez-Amaro, R., et al. 1994. Induction of tumor necrosis factor alpha production by human hepatocytes in chronic viral hepatitis. *J. Exp. Med.* **179**:841–848.
5. Leist, M., et al. 1997. Tumor necrosis factor-induced apoptosis during the poisoning of mice with hepatotoxins. *Gastroenterology.* **112**:923–934.
6. Tartaglia, L.A., Rothe, M., Hu, Y.F., and Goeddel, D.V. 1993. Tumor necrosis factor's cytotoxic activity is signaled by the p55 TNF receptor. *Cell.* **73**:213–216.
7. Rothe, J., Gehr, G., Loetscher, H., and Lesslauer, W. 1992. Tumor necrosis factor receptors: structure and function. *Immunol. Res.* **11**:81–90.
8. Banner, D.W., et al. 1993. Crystal structure of the soluble human 55 kd TNF receptor-human TNF beta complex: implications for TNF receptor activation. *Cell.* **73**:431–445.
9. Hsu, H., Xiong, J., and Goeddel, D.V. 1995. The TNF receptor 1-associated protein TRADD signals cell death and NF-kappa B activation. *Cell.* **81**:495–504.
10. Hsu, H., Shu, H.B., Pan, M.G., and Goeddel, D.V. 1996. TRADD-TRAF2 and TRADD-FADD interactions define two distinct TNF receptor 1 signal transduction pathways. *Cell.* **84**:299–308.
11. Faubion, W.A., and Gores, G.J. 1998. Death receptors in liver biology and pathobiology. *Hepatology.* **29**:1–4.
12. Chinnaiyan, A.M., et al. 1996. FADD/MORT1 is a common mediator of CD95 (Fas/APO-1) and tumor necrosis factor receptor-induced apoptosis. *J. Biol. Chem.* **271**:4961–4965.
13. Muzio, M., et al. 1996. FLICE, a novel FADD-homologous ICE/CED-3-like protease, is recruited to the CD95 (Fas/APO-1) death-inducing signaling complex. *Cell.* **85**:817–827.
14. Boldin, M.P., Goncharov, T.M., Goltsev, Y.V., and Wallach, D. 1996. Involvement of MACH, a novel MORT1/FADD-interacting protease, in Fas/APO-1- and TNF receptor-induced cell death. *Cell.* **85**:803–815.
15. Duan, H., and Dixit, V.M. 1997. RAIDD is a new "death" adaptor molecule. *Nature.* **385**:86–89.
16. Deveraux, Q.L., and Reed, J.C. 1999. IAP family proteins: suppressors of apoptosis. *Genes Dev.* **13**:239–252.
17. Van Antwerp, D.J., Martin, S.J., Kafri, T., Green, D.R., and Verma, I.M. 1996. Suppression of TNF-alpha-induced apoptosis by NF-kappaB. *Science.* **274**:787–789.
18. Wang, C.Y., Mayo, M.W., Korneluk, R.G., Goeddel, D.V., and Baldwin, A.S., Jr. 1998. NF-kappaB antiapoptosis: induction of TRAF1 and TRAF2 and c-IAP1 and c-IAP2 to suppress caspase-8 activation. *Science.* **281**:1680–1683.
19. Dbaibo, G.S., et al. 1997. Cytokine response modifier A (CrmA) inhibits ceramide formation in response to tumor necrosis factor (TNF)-alpha: CrmA and Bcl-2 target distinct components in the apoptotic pathway. *J. Exp. Med.* **185**:481–490.
20. Heller, R.A., and Kronke, M. 1994. Tumor necrosis factor receptor-mediated signaling pathways. *J. Cell Biol.* **126**:5–9.
21. Hannun, Y.A. 1996. Functions of ceramide in coordinating cellular responses to stress. *Science.* **274**:1855–1859.
22. Kronke, M., Schutze, S., Wiegmann, K., and Machleidt, T. 1996. Sphingomyelinases and TNF-induced apoptosis. *Cell. Physiol. Biochem.* **6**:337–344.
23. Monney, L., et al. 1998. Role of an acidic compartment in tumor-necrosis-factor-alpha-induced production of ceramide, activation of caspase-3 and apoptosis. *Eur. J. Biochem.* **251**:295–303.
24. Rowan, A.D., Mason, P., Mach, L., and Mort, J.S. 1992. Rat procathepsin B. Proteolytic processing to the mature form in vitro. *J. Biol. Chem.* **267**:15993–15999.
25. Roberts, L.R., et al. 1997. Cathepsin B contributes to bile salt-induced apoptosis of rat hepatocytes. *Gastroenterology.* **113**:1714–1726.
26. Jones, B., Roberts, P.J., Faubion, W.A., Kominami, E., and Gores, G.J. 1998. Cystatin A expression reduces bile salt-induced apoptosis in a rat hepatoma cell line. *Am. J. Physiol.* **275**:G723–G730.
27. Faubion, W.A., et al. 1999. Toxic bile salts induce rodent hepatocyte apoptosis via direct activation of Fas. *J. Clin. Invest.* **103**:137–145.
28. Lotem, J., and Sachs, L. 1996. Differential suppression by protease inhibitors and cytokines of apoptosis induced by wild-type p53 and cytotoxic agents. *Proc. Natl. Acad. Sci. USA.* **93**:12507–12512.
29. Nitatori, T., et al. 1995. Delayed neuronal death in the CA1 pyramidal cell layer of the gerbil hippocampus following transient ischemia is apoptosis. *J. Neurosci.* **15**:1001–1011.
30. Hill, I.E., Preston, E., Monette, R., and MacManus, J.P. 1997. A comparison of cathepsin B processing and distribution during neuronal death in rats following global ischemia or decapitation necrosis. *Brain Res.* **751**:206–216.
31. Vancompernolle, K., et al. 1998. Atractyloside-induced release of cathepsin B, a protease with caspase-processing activity. *FEBS Lett.* **438**:150–158.
32. Deussing, J., et al. 1998. Cathepsins B and D are dispensable for major histocompatibility complex class II-mediated antigen presentation. *Proc. Natl. Acad. Sci. USA.* **95**:4516–4521.
33. Xu, Y., et al. 1998. NF-kappaB inactivation converts a hepatocyte cell line TNF-alpha response from proliferation to apoptosis. *Am. J. Physiol.* **275**:C1058–C1066.
34. Iimuro, Y., et al. 1998. NFkappaB prevents apoptosis and liver dysfunction during liver regeneration. *J. Clin. Invest.* **101**:802–811.
35. Martins, L.M., et al. 1997. Activation of multiple interleukin-1beta converting enzyme homologues in cytosol and nuclei of HL-60 cells during etoposide-induced apoptosis. *J. Biol. Chem.* **272**:7421–7430.
36. Mesner, P.W.J., et al. 1999. Characterization of caspase processing and activation in HL-60 cell cytosol under cell-free conditions. *J. Biol. Chem.* **274**:22635–22645.
37. Kaufmann, S.H. 1989. Additional members of the rat liver lamin polypeptide family: structural and immunological characterization. *J. Biol. Chem.* **264**:13946–13955.
38. Fields, A.P., Kaufmann, S.H., and Shaper, J.H. 1986. Analysis of the internal nuclear matrix. Oligomers of a 38 kD nucleolar polypeptide stabilized by disulfide bonds. *Exp. Cell Res.* **164**:139–153.
39. Leist, M., Volbracht, C., Fava, E., and Nicotera, P. 1998. 1-Methyl-4-phenylpyridinium induces autocrine excitotoxicity, protease activation, and neuronal apoptosis. *Mol. Pharmacol.* **54**:789–801.
40. Yang, J., et al. 1997. Prevention of apoptosis by Bcl-2: release of cytochrome c from mitochondria blocked. *Science.* **275**:1129–1132.
41. Kawashima, A., et al. 1998. A simple procedure for the isolation of rat kidney lysosomes. *Kidney Int.* **54**:275–278.
42. Yamada, H., Hayashi, H., and Natori, Y. 1984. A simple procedure for the isolation of highly purified lysosomes from normal liver. *J. Biochem.* **95**:1155–1160.
43. Botla, R., Spivey, J.R., Aguilar, H., Bronk, S.F., and Gores, G.J. 1995. Ursodeoxycholate (UDCA) inhibits the mitochondrial membrane permeability transition induced by glycochenodeoxycholate: a mechanism of UDCA cytoprotection. *J. Pharmacol. Exp. Ther.* **272**:930–938.
44. Luo, X., Budihardjo, I., Zou, H., Slaughter, C., and Wang, X. 1998. Bid, a Bcl2 interacting protein, mediates cytochrome c release from mitochondria in response to activation of cell surface death receptors. *Cell.* **94**:481–490.
45. Squier, M.K.T., and Cohen, J.J. 1996. Calpain and cell death. *Cell Death Differ.* **3**:275–283.
46. Han, Y., Weinman, S., Boldogh, I., Walker, R.K., and Brasier, A.R. 1999. Tumor necrosis factor-inducible IB proteolysis mediated by cytosolic m-calpain. A mechanism parallel to the ubiquitin-proteasome pathway for nuclear factor-B activation. *J. Biol. Chem.* **274**:787–794.
47. Jones, B.E., et al. 2000. Hepatocytes sensitized to tumor necrosis factor-alpha cytotoxicity undergo apoptosis through caspase-dependent and caspase-independent pathways. *J. Biol. Chem.* **275**:705–712.
48. Slee, E.A., Adrain, C., and Martin, S.J. 1999. Serial killers: ordering cas-

pase activation events in apoptosis. *Cell Death Differ.* **6**:1067–1074.

49. Scaffidi, C., et al. 1998. Two CD95 (APO-1/Fas) signaling pathways. *EMBO J.* **17**:1675–1687.

50. Scaffidi, C., et al. 1999. Differential modulation of apoptosis sensitivity in CD95 type I and type II cells. *J. Biol. Chem.* **274**:22532–22538.

51. Slee, E.A., et al. 1999. Ordering the cytochrome c-initiated caspase cascade: hierarchical activation of caspases-2, -3, -6, -7, -8, and -10 in a caspase-9-dependent manner. *J. Cell Biol.* **144**:281–292.

52. Mach, L., Stuwe, K., Hagen, A., Ballaun, C., and Glossl, J. 1992. Proteolytic processing and glycosylation of cathepsin B. The role of the primary structure of the latent precursor and of the carbohydrate moiety for cell-type-specific molecular forms of the enzyme. *Biochem. J.* **282**:577–582.

53. Mach, L., et al. 1993. Activation of procathepsin B in human hepatoma cells: the conversion into the mature enzyme relies on the action of cathepsin B itself. *Biochem. J.* **293**:437–442.

54. Zhou, Q., and Salvesen, G.S. 1997. Activation of pro-caspase-7 by serine proteases includes a non-canonical specificity. *Biochem. J.* **324**:361–364.

55. Schotte, P., et al. 1998. Cathepsin B-mediated activation of the proinflammatory caspase-11. *Biochem. Biophys. Res. Commun.* **251**:379–387.

56. Lacronique, V., et al. 1996. Bcl-2 protects from lethal hepatic apoptosis induced by an anti-Fas antibody in mice. *Nat. Med.* **2**:80–86.

57. Bradham, C.A., et al. 1998. The mitochondrial permeability transition is required for tumor necrosis factor alpha–mediated apoptosis and cytochrome c release. *Mol. Cell. Biol.* **18**:6353–6364.

58. Pastorino, J.G., et al. 1996. The cytotoxicity of tumor necrosis factor depends on induction of the mitochondrial permeability transition. *J. Biol. Chem.* **271**:29792–29798.

59. Bossy-Wetzel, E., and Green, D. 1999. Caspases induce cytochrome c release from mitochondria by activating cytosolic factors. *J. Biol. Chem.* **274**:17484–17490.

60. Kuwana, T., et al. 1998. Apoptosis induction by caspase-8 is amplified through the mitochondrial release of cytochrome c. *J. Biol. Chem.* **273**:16589–16594.

61. Li, H., Zhu, H., Xu, C.J., and Yuan, J. 1998. Cleavage of BID by caspase 8 mediates the mitochondrial damage in the Fas pathway of apoptosis. *Cell.* **94**:491–501.

62. Gross, A., et al. 1999. Caspase cleaved BID targets mitochondria and is required for cytochrome c release, while BCL-XL prevents this release but not tumor necrosis factor-R1/Fas death. *J. Biol. Chem.* **274**:1156–1163.

63. Wallach, D., et al. 1997. Cell death induction by receptors of the TNF family: towards a molecular understanding. *FEBS Lett.* **410**:96–106.

64. Deiss, L.P., Galinka, H., Berissi, H., Cohen, O., and Kimchi, A. 1996. Cathepsin D protease mediates programmed cell death induced by interferon-gamma, Fas/APO-1 and TNF-alpha. *EMBO J.* **15**:3861–3870.

65. Roberg, K., Johansson, U., and Ollinger, K. 1999. Lysosomal release of cathepsin D precedes relocation of cytochrome c and loss of mitochondrial transmembrane potential during apoptosis induced by oxidative stress. *Free Radic. Biol. Med.* **27**:1228–1237.

66. Rothe, J., et al. 1993. Mice lacking the tumour necrosis factor receptor 1 are resistant to TNF-mediated toxicity but highly susceptible to infection by Listeria monocytogenes. *Nature.* **364**:798–802.

67. Wang, J., et al. 1999. Inherited human caspase 10 mutations underlie defective lymphocyte and dendritic cell apoptosis in autoimmune lymphoproliferative syndrome type II. *Cell.* **98**:47–58.

68. Kawahara, A., Ohsawa, Y., Matsumura, H., Uchiyama, Y., and Nagata, S. 1998. Caspase-independent cell killing by Fas-associated protein with death domain. *J. Cell Biol.* **143**:1353–1360.